Ecology, 98(5), 2017, pp. 1239–1255

Predicting trait-environment relationships for venation networks along an Andes-Amazon elevation gradient

Benjamin Blonder,[1,10] Norma Salinas,[1,2] Lisa Patrick Bentley,[1] Alexander Shenkin,[1] Percy O. Chambi Porroa,[3] Yolvi Valdez Tejeira,[3] Cyrille Violle,[4] Nikolaos M. Fyllas,[1] Gregory R. Goldsmith,[5] Roberta E. Martin,[6] Gregory P. Asner,[6] Sandra Díaz,[1,7] Brian J. Enquist,[8,9] and Yadvinder Malhi[1]

[1]*Environmental Change Institute, School of Geography and the Environment, University of Oxford, Oxford, OX1 3QY UK*
[2]*Sección Química, Pontificia Universidad Católica del Perú, San Miguel, Lima, Peru*
[3]*Universidad Nacional de San Antonio Abad del Cusco, Cusco, Peru*
[4]*Centre d'Ecologie Fonctionnelle et Evolutive (UMR 5175), CNRS, Université de Montpellier, Université Paul Valéry Montpellier, EPHE, Montpellier, France*
[5]*Ecosystem Fluxes Group, Laboratory for Atmospheric Chemistry, Paul Scherrer Institute, Villigen, 5232 Switzerland*
[6]*Department of Global Ecology, Carnegie Institution for Science, Stanford, California 94305 USA*
[7]*Instituto Multidisciplinario de Biología Vegetal (IMBIV, CONICET-UNC) and FCEFyN, Universidad Nacional de Córdoba, Cordoba, Argentina*
[8]*Department of Ecology and Evolutionary Biology, University of Arizona, Tucson, Arizona 85721 USA*
[9]*The Santa Fe Institute, 1399 Hyde Park Rd, Santa Fe, New Mexico 87501 USA*

Abstract. Understanding functional trait-environment relationships (TERs) may improve predictions of community assembly. However, many empirical TERs have been weak or lacking conceptual foundation. TERs based on leaf venation networks may better link individuals and communities via hydraulic constraints. We report measurements of vein density, vein radius, and leaf thickness for more than 100 dominant species occurring in ten forest communities spanning a 3,300 m Andes-Amazon elevation gradient in Peru. We use these data to measure the strength of TERs at community scale and to determine whether observed TERs are similar to those predicted by physiological theory. We found strong support for TERs between all traits and temperature, as well weaker support for a predicted TER between maximum abundance-weighted leaf transpiration rate and maximum potential evapotranspiration. These results provide one approach for developing a more mechanistic trait-based community assembly theory.

Key words: abundance-weighting; Amazon basin; Andes; community assembly; community-weighted mean; conductance; environmental filtering; functional trait; leaf thickness; trait-environment relationship; vein density; vein radius.

Introduction

A major goal of trait-based ecology is to use simple measurements of traits to create and inform predictive models of community assembly (Lavorel and Garnier 2002, McGill et al. 2006, Violle et al. 2014). The performance of different traits should vary within environment (Weiher and Keddy 1999, Suding et al. 2008), because of either physiological limitations, species interactions (Cody and Diamond 1975, Connor and Simberloff 1979), or historical/stochastic processes not related to traits (Vellend and Agrawal 2010, Fukami 2015). In the first two cases, selection should lead to filtering of species by response trait values along environmental gradients (Díaz et al. 1998, Shipley et al. 2006, Weiher et al. 2011) and thus differential community assembly along environmental gradients. Integrating these ideas into predictive community ecology requires progress in two key areas: identifying empirical trait-environment relationships (TERs) and developing theory to quantitatively predict them.

Establishing strong empirical TERs has been challenging. Abundance-weighted functional trait distributions may show the clearest response to climate because of stronger filtering on common species (Cingolani et al. 2007) and the centrality of common species in trait space (Umaña et al. 2015). However, both weighted and unweighted patterns are often weak. For example, the global leaf economics spectrum (Wright et al. 2004) shows stratification across biomes (Reich et al. 1999, Wright et al. 2005), but large fractions of the global range of ecological strategies are represented within any local community (Wright et al. 2004, Elser et al. 2010, Blonder et al. 2013, Edwards et al. 2014). Similarly, neither temperature nor precipitation could explain more than 29% of the variance in 21 different traits (Moles et al. 2014). Indeed, individual traits thought to have major ecological importance, that are often used as proxies for overall growth strategy (Craine 2009, Reich 2014), also show highly variable and often weak or opposite relationships among species and locations (e.g., leaf mass per area Read et al. 2014).

Manuscript received 14 September 2016; revised 30 November 2016; accepted 11 January 2017. Corresponding Editor: Jeannine Marie Cavender-Bares.
[10]E-mail: bblonder@gmail.com

Some stronger relationships have unclear origins. In paleoclimate reconstruction, the fraction of species with toothed vs. entire leaves within a community predicts community temperature (Bailey and Sinnott 1915, Peppe et al. 2011), while a wider set of leaf morphological variables has been used to reconstruct other climate variables (Wolfe 1993, Royer et al. 2005). However, the underlying processes often remain unknown (but see Royer and Wilf 2006), or are driven by the colonization of large regions by clades showing phylogenetic niche conservatism (Little et al. 2010, Hinojosa et al. 2011). As a result, trait-environment relationships may vary unpredictably across regions if relationships are primarily driven by shared biogeographic history and phylogenetic position rather than species sorting based on the function of that trait. Such effects limit our ability to use traits to predict the composition of communities in response to novel environmental conditions because of ambiguity about underlying processes and the need to make out-of-sample predictions (Jackson and Overpeck 2000, Jordan 2011).

In addition to the challenges associated with discerning strong TERs, there is limited theory that can quantitatively predict them. The strongest approach would be to establish mechanistic linkages between traits and performance, then between performance and fitness across environmental contexts, which could be solved to direct predict relationships between traits and environment (Arnold 1983). There are a small number of models for plant performance that are based on environmental forcing of individuals with different trait combinations (Thornley 1991, Scheiter et al. 2013, Fyllas et al. 2014), or based on couplings between hydraulics and environment (Tyree and Sperry 1988, Bartlett et al. 2012, Manzoni et al. 2013, Martínez-Vilalta et al. 2014). In other cases, models exist that can predict trait values, e.g., for leaf hydraulics (de Boer et al. 2012, Blonder and Enquist 2014), but the last stage - explicit linkages to fitness and environment - is lacking. As a result, making mechanistic linkages between traits and environment remains generally challenging.

Many ecological models remain largely conceptual rather than quantitative (Houlahan 2016). Conceptual models are those that yield non-specific predictions, e.g., a positive relationship between A and B that can be assessed by using linear regression. Such a model can be assessed by proposing a form $Y = AX+B$ and fitting values of coefficients A and B, then determining if they are different than zero. In contrast, quantitative models are those that propose a fully determined model, e.g., $Y = AX+B$ where the values of A and B take specific predicted numerical values. Such a model can be assessed by determining how observed values of Y differ from predictions. The key difference is that in the former case, the coefficients and form of the model are discovered from the test data; in the latter, both are predicted independent of the test data (Marquet et al. 2014). Such quantitative predictions are common in physics (e.g., the orbit of a planet in a gravitational field), but have been more difficult in the more complex systems characterizing community ecology (Levins 1966, Levins and Lewontin 1985).

Here we ask how leaf venation network traits are coupled to the environment. The motivation for exploring vein traits is the broad evidence indicating that these networks are ecophysiologically linked to plant response to environment. Veins supply the water lost via transpiration through stomata, with denser venation leading to increased hydraulic conductance (Roth-Nebelsick et al. 2001). In general, there is a coupling between hydraulic conductance and stomatal conductance so that water supply and demand are matched (Brodribb and Jordan 2011). Because higher stomatal conductance enables higher rates of carbon assimilation (Brodribb et al. 2007), selection against plants with certain water-use or carbon-gain strategies could result in environmental filtering on a suite of venation network traits. Consistent with this idea, venation network TERs generally appear to be strong and have been described for environmental gradients at both interspecific (Uhl and Mosbrugger 1999, Kessler et al. 2007, Sack and Scoffoni 2013, Blonder et al. 2016) and intraspecific (Blonder et al. 2013) scales. At the community scale, this pattern also appears to hold in New World tropical forests and temperate subalpine/alpine environments, with limited phylogenetic niche conservatism observed in venation network traits (Blonder and Enquist 2014). At longer macroevolutionary time scales, there is also evidence for TERs between global environmental change and novel network geometries, e.g., across the Cretaceous (Boyce et al. 2009, Brodribb and Feild 2010).

A key composite trait for leaf venation networks is hydraulic path length, which determines the maximum distance between the epidermis and any vein (Fig. 1). This variable is a function of several traits including leaf inter-vein maximum distance (IVD, mm), leaf thickness (d_y, mm), and vascular bundle radius (r_v, mm). Lower hydraulic path lengths have been shown to predict higher leaf hydraulic conductance (Brodribb et al. 2007), although several other anatomical variables, discussed in the Methods, are also implicated. IVD is mathematically related to a commonly measured trait, vein density (VD; mm^{-1}), by the relationship VD * IVD = k, where k is a number that depends on areole geometry, and can be shown based on planar geometry to take a limited range of values $1 \leq k \leq 2$ (Blonder et al. 2011).

TER theory focused on paleoclimate reconstruction has been developed to predict community climate based on community-weighted mean venation traits (Blonder and Enquist 2014). The hypothesis is that maximum leaf transpiration rate (E_{max}) (a function of hydraulic conductance and thus venation network traits) should be proportional to maximum potential evapotranspiration (α PET_{max}), where α is a Priestley-Taylor coefficient. This model was algebraically solved using simple quantitative sub-models for E_{max}, α, and PET_{max} that predicted a nonlinear function for the relationship between VD and air temperature. This prediction was supported in both tropical and temperate sites (Blonder and Enquist 2014), although

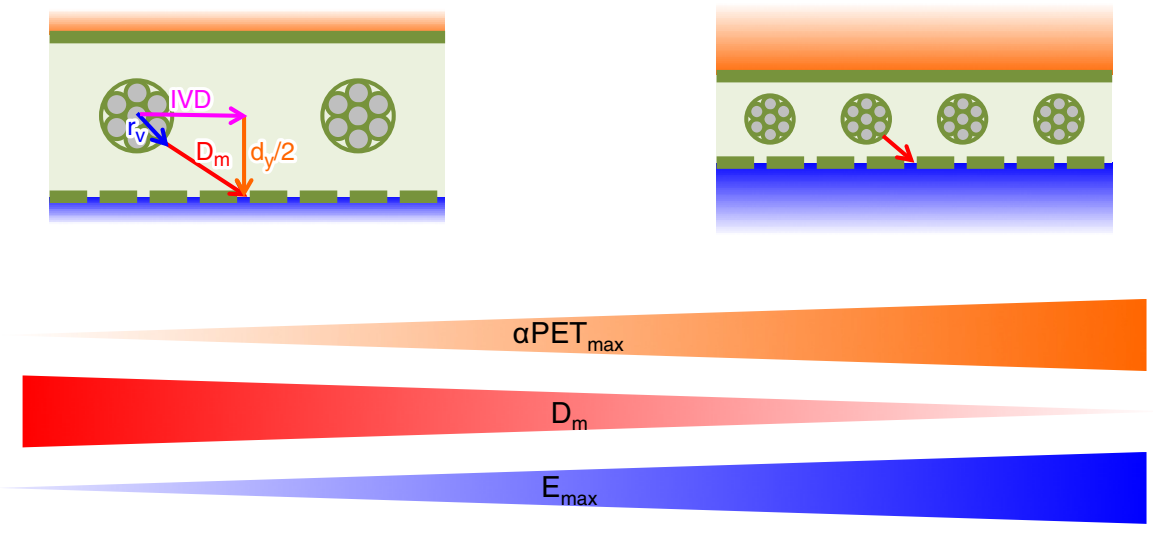

FIG. 1. Conceptual diagram of a proposed trait-environment relationship. Intervein maximum distance (IVD), vein radius (r_v), and leaf thickness (d_y) combine geometrically to determine the hydraulic path length, D_m. Lower values of D_m reduce the distance water travels between a vein and an evaporative surface, and thus increase the maximum hydraulic conductance. Higher conductance can in turn increase the maximum transpiration rate (E_{max}). The model proposes that when potential evapotranspiration ($\alpha\,PET_{max}$; above-leaf gradient) in the environment is high, E_{max} should also be high (below-leaf gradient), driving lower values of D_m. Variation in D_m can be achieved by variation in VD, r_v, d_y, and other anatomical traits. [Colour figure can be viewed at wileyonlinelibrary.com]

both similar and opposite empirical patterns have been found in some clades (Mason and Donovan 2015, Blonder et al. 2016). An open question is whether this theory can also provide an approach for predicting community-weighted venation network traits from climate.

To move towards more predictive understandings of TERs, we present an empirical study of a 3,300 m elevation gradient in eastern Peru. Venation network traits for Andean and Amazonian species and communities have been poorly described, despite the high regional biodiversity. We report empirical patterns of abundance and venation network trait variation in more than 100 dominant angiosperm tree species in ten 1-ha plots. We then use these data to describe the strength of empirical TERs involving venation network traits at community scale, to critically compare observations to expected TERs predicted by the vein-climate model, and to examine phylogenetic structure in observed relationships.

METHODS

Study site

This study included 10 plots that belong to a group of permanent 1-ha plots along elevation gradients in the departments of Cusco and Madre de Dios in SE Peru. A detailed map of these plots can be found in Malhi et al. (*in review*). Six of the plots are montane plots in the Kosñipata Valley, spanning an elevation range 1500–3500 m (Malhi et al., 2010), two are submontane plots located in the Pantiacolla front range of the Andes (range 600–900 m) and two plots are found in the Amazon lowlands in Tambopata National Park (elevation range 200–225 m). The elevation gradient is very moist (Table 1), with seasonal cloud immersion common above 1,500 m elevation (Halladay et al. 2012).

The plots are part of a long-term research effort coordinated by the Andes Biodiversity Ecosystems Research Group (ABERG, http://www.andesconservation.org) and are part of the ForestPlots (https://www.forestplots.net/) and Global Ecosystems Monitoring Network (GEM; http://gem.tropicalforests.ox.ac.uk/projects/aberg) networks. Plots were established between 2003 and 2013 in areas that have relatively homogeneous soil substrates and stand structure, as well as minimal evidence of human disturbance (Girardin et al. 2014*a*).

Census and abundance data

Within each plot, all stems ≥10 cm diameter at breast height were tagged, sized, and identified to species-level by William Farfan and Miles Silman during a 2013 or the most recent year before 2013 tree census, and then recorded in the ForestPlots database (https://www.forestplots.net). A subset of these stems were selected based on their abundance for trait sampling. These individuals were examined and potentially renamed by taxonomic experts at the Carnegie Institution for Science (https://cao.carnegiescience.edu/spectranomics) (Malhi et al., *in review*). Abundances for each taxon within each plot were then calculated using the revised names as summed basal area across all stems.

TABLE 1. Characteristics of communities sampled along the Kosñipata tropical forest elevation gradient. Trait columns indicate abundance-weighted means and standard deviations. Columns "species/branches measured" refer to the number of units for which angiosperm trait measurements were available.

Plot code	Latitude (°)	Longitude (°)	Elevation (m)	MAT (°C)	MAP (mm yr^{-1})	αPET (mmol $m^{-2} s^{-1}$)	VD (mm^{-1})	IVD (mm)	r_v (mm)	d_v (mm)	E_{max} (mmol $m^{-2} s^{-1}$)	No. branches measured	No. species measured
TAM-06	−12.8385	−69.296	215	24.4	1,900	8.09	10.883 ± 4.570	0.129 ± 0.060	0.041 ± 0.014	0.221 ± 0.047	2.824 ± 2.020	75	21
TAM-05	−12.8309	−69.2705	223	24.4	1,900	8.08	14.318 ± 2.496	0.084 ± 0.020	0.034 ± 0.008	0.192 ± 0.032	4.350 ± 2.347	80	24
PAN-02	−12.6495	−71.2626	595	23	2,366	9.19	15.294 ± 3.870	0.077 ± 0.028	0.038 ± 0.006	0.218 ± 0.040	5.997 ± 4.382	55	12
PAN-03	−12.6383	−71.2744	859	21.9	2,835	8.92	12.758 ± 2.639	0.097 ± 0.024	0.037 ± 0.006	0.236 ± 0.061	3.779 ± 2.565	58	13
SPD-02	−13.0491	−71.5365	1,494	18.8	5,302	7.18	14.850 ± 3.451	0.077 ± 0.027	0.036 ± 0.011	0.205 ± 0.040	5.165 ± 1.997	92	23
SPD-01	−13.0475	−71.5423	1,713	17.4	5,302	7.02	12.092 ± 3.097	0.102 ± 0.037	0.044 ± 0.013	0.304 ± 0.099	3.443 ± 1.477	114	26
TRU-04	−13.1055	−71.5893	2,719	13.5	2,318	8.15	11.103 ± 3.175	0.121 ± 0.057	0.042 ± 0.008	0.367 ± 0.138	2.349 ± 0.781	95	15
ESP-01	−13.1751	−71.5948	2,868	13.1	1,560	6.41	9.992 ± 2.221	0.132 ± 0.056	0.047 ± 0.010	0.407 ± 0.095	2.060 ± 0.703	93	12
WAY-01	−13.1908	−71.5874	3,045	11.8	1,560	6.24	8.995 ± 3.312	0.162 ± 0.077	0.055 ± 0.011	0.559 ± 0.210	1.718 ± 0.856	74	12
ACJ-01	−13.14689	−71.6323	3,537	9	1,980	6.65	10.175 ± 3.513	0.144 ± 0.067	0.044 ± 0.006	0.419 ± 0.123	1.945 ± 0.883	75	9

Trait sampling approach

From April–November 2013, we measured plant traits as part of the CHAMBASA (CHallenging Attempt to Measure Biotic Attributes along the Slopes of the Andes) project. Based on census data for 2013 or the most recent census year before 2013, a sampling protocol was adopted wherein species were sampled that maximally contributed to plot basal area (a proxy for plot biomass or crown area). We aimed to sample the minimum number of species that contributed to 80% of basal area, although in the diverse lowland forest plots we only sampled species comprising 60–70% of plot basal area. Within each sampled species in each plot, five trees in upland sites and three trees in lowland sites were chosen for sampling. If three trees were not available in the chosen plot, we sampled additional individuals of the same species from an area immediately surrounding the plot. Using single rope tree climbing techniques, we sampled one fully sunlit canopy branch and a fully shaded branch where possible, each at least 1 cm diameter, from each tree. Across all plots, approximately 40% of trees had also shade branches sampled (some trees had no shade branches available). From each branch, we measured five leaves from simple-leaved species, or five individual leaflets from compound-leaved species (both referred to as "leaf" below) for trait measurements. Branches and leaves with minimal damage were chosen.

For this study, data are reported for only angiosperms, because the TER model described below is not necessarily applicable to gymnosperms and ferns with differing physiologies. However angiosperms do comprise the overwhelming majority of biomass and number of individuals across these plots (Malhi et al. *in review*).

Trait measurements

Area shrinkage (S; m^2 m^{-2}).—We calculated the fraction of leaf area that was lost upon drying (varying from 0 to 1). We used the supplementary data provided by Blonder et al. (2012) to calibrate a leaf-level shrinkage using a random forest regression model with leaf mass per area, fresh lamina area and leaf thickness as predictor variables. This model explained 46.6% of the variation in the calibration data. On application to leaves from this dataset, it yielded shrinkage values of S = 0.12 ± 0.05 SD.

Leaf thickness (d_v; mm).—We measured the thickness of each leaf in the field immediately after collection using a micrometer (Tresna, 211-101F). Measurements were taken on the lamina, avoiding primary, secondary, and tertiary veins.

Vein density and intervein distance (VD, mm^{-1}; IVD, mm).—Using pressed dried leaf material, we prepared a slide-mount of each leaf's venation network following standard chemical clearing and staining protocol, with leaf epidermal layers removed using a small brush

(Pérez-Harguindeguy et al. 2013). We then photographed each slide-mounted leaf using a Olympus SZX-12 microscope with transillumination and coupled to a Canon T1i digital camera. Images were obtained with a final resolution of 179 pixels mm^{-1}, with a full extent of 12.8 mm × 19.3 mm. Images were enhanced using in MATLAB by applying contrast limited adaptive histogram equalization to the green channel of each image, using a sliding window of 200 pixels and a gain of 0.01. We traced all veins within a well-cleared polygonal region of interest of each image (mean area 36 ± 23 SD mm^2). We calculated VD_{raw} in MATLAB by dividing the total length of the skeletonized traced veins by the total area of the region of interest. We calculated IVD_{raw} by performing a Euclidean distance transformation on the skeletonized image. Within each areole, the maximum of this distance transformation is equivalent to the maximum distance from a vein. We then calculated IVD_{raw} as the mean of this distribution. We then corrected raw measurements for shrinkage using a factor using the relationship between areal and linear scales as

$$\begin{aligned} \mathrm{VD} &= \mathrm{VD}_{\mathrm{raw}} \cdot \frac{1}{\sqrt{1-S}} \\ \mathrm{IVD} &= \mathrm{IVD}_{\mathrm{raw}} \cdot \sqrt{1-S} \end{aligned} \tag{1}$$

Vein radius (r_v; mm).—On each cleared leaf image, we randomly selected 50 vein segments from the ultimate venation network with a MATLAB program. We then measured the maximum diameter of each vein segment using a software ruler tool and calculated a raw diameter as the median of this distribution ($r_{v,\mathrm{raw}}$; mm) for each image. We then multiplied by a shrinkage factor, yielding

$$r_v = r_{v,raw} \cdot \sqrt{1-S}. \tag{2}$$

Hydraulic path length (D_m; μm).—We estimated the approximate hydraulic path length for water flow away from veins through the mesophyll towards an evaporative surface via apoplastic pathways (Fig. 1) as

$$D_m \approx \sqrt{X^2 + Y^2}. \tag{3}$$

Here X and Y are horizontal and vertical distances through the mesophyll via apoplastic pathways. Following (Brodribb et al. 2007), we assume that individual cells have dimensions C_x and C_y.These terms then can be written as

$$\begin{aligned} X &= v \cdot \frac{(C_x - C_y) + C_y \cdot (\pi/2)}{C_x} \\ Y &= t \cdot \frac{\pi}{2} \end{aligned}. \tag{4}$$

Here v and t are distances that can be related to functional traits as

$$\begin{aligned} v &= 1000\left(\mathrm{IVD} - r_v \cos\theta\right) \\ t &= 1000\left(\frac{d_y}{2} - r_v \sin\theta\right) \end{aligned} \tag{5}$$

parsimoniously assuming that veins are located halfway between the abaxial and adaxial surface of the leaf, where θ is the angle between the plane of the leaf and the origin point of the maximum-length minimum path from the vein to the epidermis, and where the factor of 1,000 converts mm to μm. An exact but complex expression for θ can be found by solving for $\frac{dD_m}{d\theta} = 0$, or alternatively, an approximate solution can be obtained assuming that the maximum-length path proceeds between the horizontal and vertical, i.e., θ = π/4. Eq. 3 therefore simplifies to

$$D_m = 1000 \sqrt{\frac{\pi^2}{4}\left(\frac{d_y}{2} - \frac{r_v}{\sqrt{2}}\right)^2 + \left(1 + \frac{C_y}{C_x}\left(\frac{\pi}{2} - 1\right)\right)^2 \left(\mathrm{IVD} - \frac{r_v}{\sqrt{2}}\right)^2}. \tag{6}$$

Estimated leaf hydraulic conductance (K_{est}; mmol H_2O m^{-2} s^{-1} MPa^{-1}).—We estimated maximum leaf hydraulic conductance following the data of Brodribb et al. (2007) as

$$K_{\mathrm{est}} = 12670 \cdot {D_m}^{-1.26}. \tag{7}$$

Leaf hydraulic conductance also depends on several physiological and environmental variables beyond venation network traits such as xylem conduit number/size, bundle sheath anatomy, etc. (Rockwell et al. 2014, Buckley et al. 2015, Simonin et al. 2015). However, the model of Eq. 7 fits a wide set of species and does not require additional labor-intensive anatomical measurements. It therefore provides a first approximation for how venation networks constrain water flow within a leaf.

Gap-filling.—A small number (<10%) of trait measurements for leaf mass per area, fresh lamina area, and d_y were missing at random. We filled missing values using multiple imputation via chained equations, with predictive mean matching. We imputed 10 datasets for a matrix including these variables, plot code and sun/shade status. We then used mean values across these replicates to gap-fill missing observations in the original data matrix.

A physiological model for TERs

We tested a simplified version of the Blonder and Enquist (2014) TER model. This model proposed that leaves have a physiological capability for transpiration that matches the climate-determined potential evapotranspiration in the leaf's microenvironment. This model effectively assumes that the capacity for high

transpiration rates can be adaptive in terms of supporting carbon assimilation under some environmental conditions. The model in its most general form can be expressed as

$$E_{\max} = \alpha \mathrm{PET}_{\max} \quad (8)$$

where $E_{\max}$ is maximum leaf transpiration rate, α is a Priestley-Taylor coefficient that depends climate and forest structure (Priestley and Taylor 1972), and $\mathrm{PET}_{\max}$ is maximum potential evapotranspiration. The model's does not include a correction for leaf area index because the water supply-demand matching is assumed to occur at leaf scale.

The original presentation of the model expanded $\alpha\mathrm{PET}_{\max}$ into a set of nonlinear terms that could be related to latitude, temperature, [CO2], and a range of other leaf physiological variables, e.g., optimal stomatal control parameters. Most of these parameters were originally assumed to take constant values, despite evidence that they empirically vary across contexts and potentially co-vary with each other. The rationale for this choice was that the model was built for reconstructing paleoclimate, i.e., inferring climate from traits. In this context, only a small set of venation traits would be available from fossils and all other model parameters would be unknown.

However, this parameter-heavy approach can be criticized in the present context of predicting community trait distributions from climate, i.e., in exploring how environmental filtering on traits may drive community assembly. In this case much of complexity of the original model presentation can be avoided, because $\alpha\mathrm{PET}_{\max}$ can be directly calculated from weather station data. We build directly on the model's fundamental Eq. 8, and assume that $\alpha\mathrm{PET}_{\max}$ is a measured quantity, and that maximum transpiration can be expressed as the product of $K_{\mathrm{est},}$ the hydraulic conductance, and $\Delta\Psi_{ls}$, the water potential gradient from stem xylem to leaf (Sack and Holbrook 2006) under maximum transpiration conditions. This yield the relationship:

$$E_{\max} = K_{\mathrm{est}} \cdot \Delta\Psi_{ls} = \alpha \mathrm{PET}_{\max}. \quad (9)$$

Combining Eqs 7–10, a simplified TER is obtained as:

$$E_{\max} = \frac{12670 \cdot \Delta\Psi_{ls}}{1000^{1.26}} \cdot \frac{1}{\left(\frac{\pi^2}{4}\left(\frac{d_y}{2} - \frac{r_v}{\sqrt{2}}\right)^2 + \left(1 + \frac{C_y}{C_x}\left(\frac{\pi}{2} - 1\right)\right)^2 \left(\mathrm{IVD} - \frac{r_v}{\sqrt{2}}\right)^2\right)^{0.63}} = \alpha \mathrm{PET}_{\max}. \quad (10)$$

Equation 11 predicts that, all else being held constant, sites with higher potential evapotranspiration should have higher vein density or lower inter-vein distance, large vein radii, and/or lower leaf thicknesses.

There are an infinite number of ways for the venation traits to satisfy Eq. 10. As such, r_v, d_y, and VD or IVD are all potentially mutually uncorrelated. However natural selection may lead to correlations between these variables (Blonder et al. 2013). For example, some species may have high r_v to provide resistance to herbivory, while others may have high d_y to provide additional water capacitance. Alternatively, variables may be coordinated because of selection on integrated phenotypes. For example, optimal water transport should lead to an even supply of water throughout the leaf, suggesting that regions between or above the leaf veins should not be oversupplied or undersupplied (Fig. 1; Noblin et al. 2008). Assuming that veins are located midway between the upper and lower surfaces of the leaf (not always the case but a useful approximation Wylie 1946), this leads to the prediction that

$$\mathrm{IVD} = \frac{d_y}{2}. \quad (11)$$

If this relationship holds, then the dimensionality of the trait space will be reduced, and $\alpha\ \mathrm{PET}_{\max}$ becomes a function of only IVD and r_v.

Model parameterization

We explored the consequences of variation in the two unmeasured parameters of Eq. 10: C_y/C_x and $\Delta\Psi_{ls}$. Both are labor-intensive to measure and not commonly available for broad comparative studies. Under the high-transpiration conditions for which the model would apply, $\Delta\Psi_{ls}$ should take a range of values across species varying from approximately 0.2 to 1.0 MPa, with most values skewed to the lower end of this range (Choné et al. 2001, Brodribb et al. 2002, Franks 2006, Simonin et al. 2015). We therefore modeled it as being uniformly distributed as

$$\Delta\Psi_{ls} \sim U(0.2, 1.0). \quad (12)$$

Similarly, C_y/C_x can take a range of positive values. We used the 25–75% quantile range from (Brodribb et al. 2007), leading to the assumed distribution:

$$\frac{C_y}{C_x} \sim U(1, 20). \quad (13)$$

We drew 1,000 values from each of these prior distributions and used these in Eq. 10 to estimate the 25%, 50%, and 75% quantiles of the posterior distribution of E_{est}.

Community-weighting traits

Trait distributions for IVD and VD, d_y, r_v, and the quantiles of E_{est} at each site were community-weighted by

species' abundance, as measured by summed basal area across all stems (Table 1). We also repeated calculation of community-weighted means using only sun leaves and using only shade leaves.

The weight was defined as w_{ij}, for each site i and for each species $j \leq J_i$, where J_i is the total number of species in plot i. We also calculated T_{im}, the species-at-site mean values of trait T for the subset of species $\{m_i\} \subset \{1, \ldots, J_i\}$ in plot i for which trait data were available.

The weighted mean value of T in plot i was calculated as:

$$\hat{\mu}_i = \frac{\sum_{m \in \{m_i\}} w_{im} T_{im}}{\sum_{m \in \{m_i\}} w_{im}}. \quad (14)$$

Note that because $\left|\{m_i\}\right| < J_i$, this estimator is potentially biased by the trait values of species that are in the community, but were unmeasured either because their abundance or biomass was low or because trait measurements were unavailable. However, simulation studies suggest that our approach leads to <5% difference in means and <20% difference in variance at our 80% biomass sampling intensity (Paine et al. 2015).

Climate data

We obtained climate data from a set of weather stations located adjacent to each one of the study sites (Table 1). The most complete annual time series for most weather stations were for year 2013 and incoming radiation, temperature, precipitation, and relative humidity were recorded at 30-min intervals. We used these time series to estimate the average daily climate. For days that the diurnal profile was not available, the average daily values were obtained by interpolating the daily parameters of the previous and following 3 d. Because of poor humidity sensor performance at TRU-04, we estimated relative humidity there following a calibration based on dewpoint temperature at WAY-01 using the methods of Ephrath et al. (1996).

Daily total αPET was estimated within the climate submodel of the Trait-based Forest Simulator model (Fyllas et al. submitted) at each site using the Priestley-Taylor (PT) model and neglecting the heat flux into the ground (Priestley and Taylor 1972), with additional daily parameters estimated following Allen et al. (1998). We corrected temperature for altitudinal differences using an adiabatic rate of 5.5°C/km (Girardin et al. 2014*b*) and assumed no change of radiation and precipitation with altitude. We then estimated a maximum annual value, αPET_{max}, as the daily maximum value of αPET. We converted units to mmol m^2 s^{-1} from mm d^{-1} via a multiplicative factor of 1.285 = 24/12 * 10^6/18.01/86400, where the factor of 24/12 accounts for evapotranspiration only occurring during approximately 12/24 daylight hours and all other factors represent the direct unit conversion.

Phylogenetic analysis

We constructed a phylogenetic tree for all species for which trait measurements were obtained using standardized names. Voucher specimens can be viewed at https://cao.carnegiescience.edu/spectranomics using the branch codes in Data S2**.** We built the phyogenetic tree using the *phylomatic* function in Phylocom 4.2 (Webb et al. 2008) using the "R20120829" megatree. We then calculated approximate crown ages for each clade using Phylocom's *bladj* function, with constraints for internal nodes originally provided by (Wikström et al. 2001) and corrected for file transcription errors by Gastauer and Meira-Neto (2013). We then assigned trait values to the tips of this tree by calculating mean trait values across all branches and sites for which a measurement was available.

Statistical analyses

We conducted all analyses in R version 3.2.2. Phylogenetic analyses were conducted with the *ape*, *picante*, and *phytools* packages; hierarchical variance partitioning with the *nlme* package following Messier et al. (2010); random forest regression with the *randomForest* package, SMA regression with the *smart* package.

Results

Climate variation

Across the 3,300 m elevation transect, annual temperatures varied from 9.0 to 24.4°C; annual precipitation from 1,560 to 5,300 mm, and maximum daily potential evapotranspiration from 6.2 to 9.2 mmol m^{-2} s^{-1}. Elevation predicted temperature (R^2 = 0.99) and α PET_{max} (R^2 = 0.68), but not precipitation (R^2 = 0.02).

Range of trait variation

Our final dataset included trait measurements for 811 leaves from 130 taxa. This reflected collections at each site of 17 ± 6 SD species and 81 ± 18 SD branches (Table 1). All venation network traits showed extensive variation. Vein density (VD) varied from 4.8 mm^{-1} for *Clusia alata* (Clusiaceae) to 21.7 mm^{-1} for *Pourouma bicolor* (Urticaceae) (Fig. 2), while IVD showed inverse variation, from 0.043 mm for *Pourouma bicolor* to 0.277 mm for *Clusia alata*. Median minor vein radius (r_v) varied from 0.018 mm in *Rauvolfia leptophylla* (Apocynaceae) to 0.07 mm in *Clusia alata* (Clusiaceae). Leaf thickness (d_y) varied from 0.128 mm in *Rinorea viridiflora* (Violaceae) to 0.805 mm in *Clusia flaviflora* (Clusiaceae). Boxplots of trait distributions across individuals within each species and plot are available for VD (Appendix S1: Fig. S1), IVD (Appendix S1: Fig. S2), r_v (Appendix S1: Fig. S3), and d_y (Appendix S1: Fig. S4).

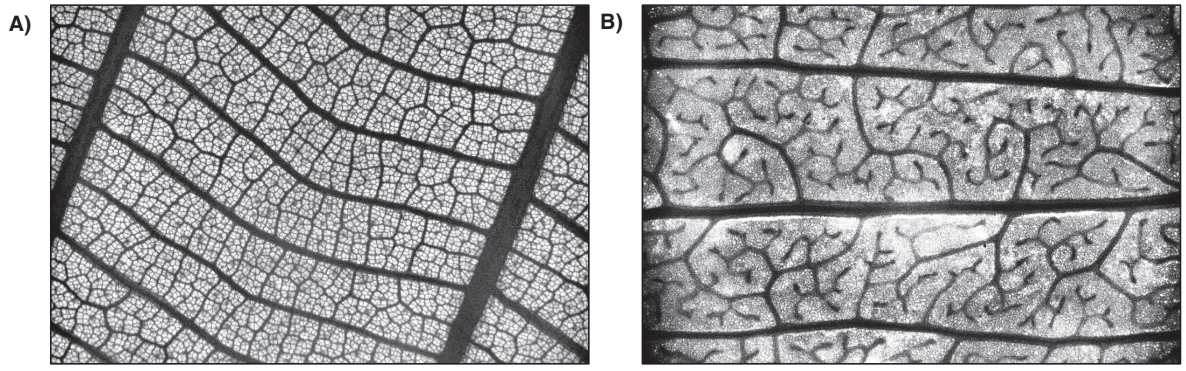

FIG. 2. Venation network traits vary widely along the elevation gradient, including leaves from species such as (A) *Pourouma bicolor* (Urticaceeae) with VD = 22.8 mm^{-1} and (B) *Clusia alata* (Clusiaceae), with mean VD = 4.0 mm^{-1}. Dimensions for each image are 19.3 mm × 12.8 mm.

There also were statistically significant, but biologically small, shifts in some venation network traits across canopy vs. shade light environments. When considering the distribution of differences between sun means and shade means for each taxon at each site, r_v was higher in the sun (mean shift 0.001 mm, $P = 0.002$), d_y was higher in the sun (mean shift 0.025 mm, $P < 10^{-6}$) and IVD was lower in the sun (mean shift −0.003 mm, $P < 0.03$). The distribution of VD did not significantly shift with light (Fig. 3).

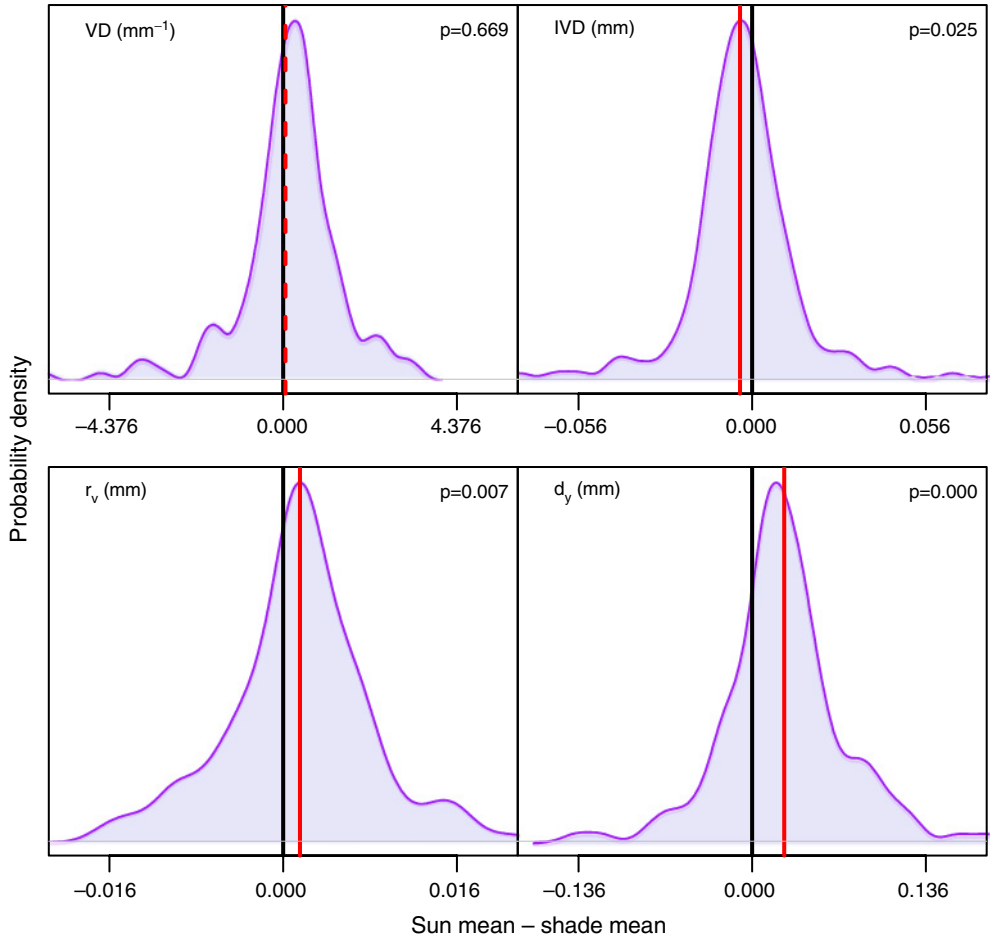

FIG. 3. Variation in venation traits across light environments. Filled distributions indicate the distribution of sun mean minus shade mean values within each species, across all species-sites combinations. The null expectation of zero is shown as a black line. The mean of the observed distribution is shown as a solid light vertical line if significantly different from zero and dashed light line if not. [Colour figure can be viewed at wileyonlinelibrary.com]

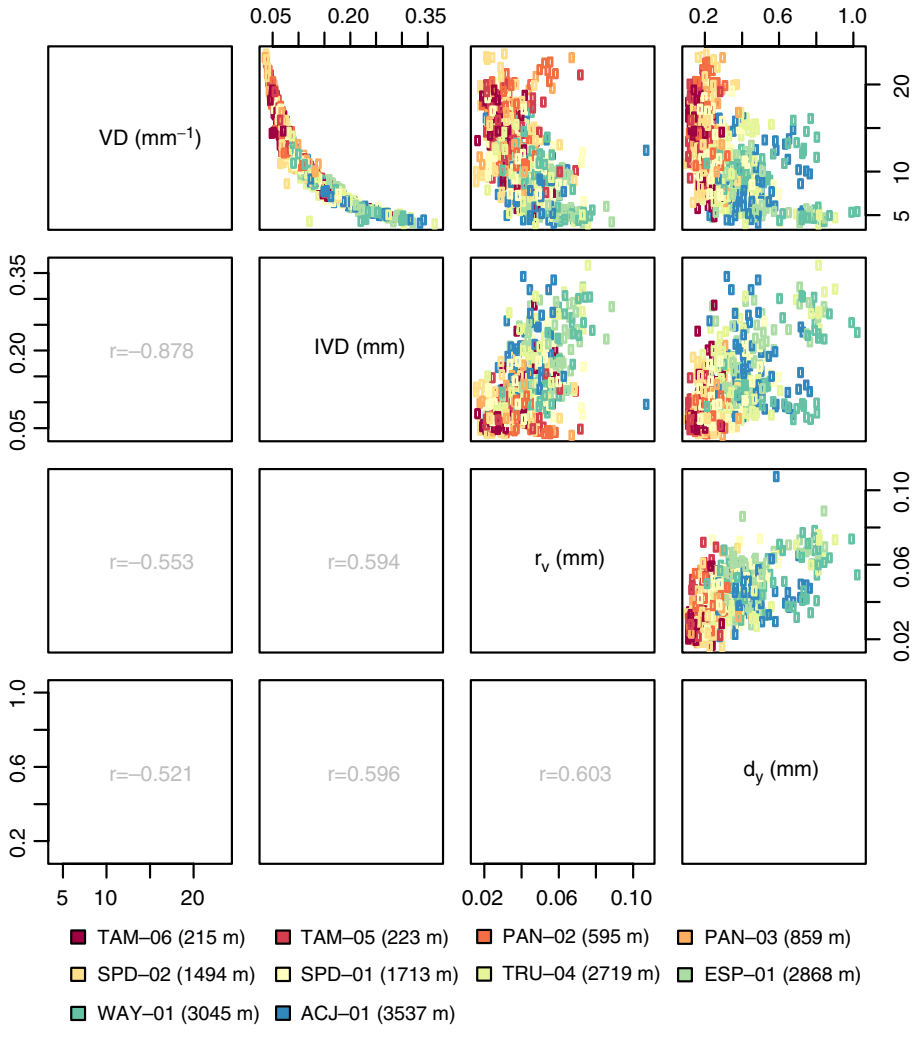

FIG. 4. Venation network trait-trait correlations. Upper panels show pairs plots, with points representing individual leaves shaded by plot elevation. Lower panels show Pearson correlation coefficients. For phylogenetic regression see Appendix S1: Table S1.

Trait intercorrelations

The venation network traits were intercorrelated with each other. At the leaf-level, higher VD was generally associated with lower r_v, and lower d_y. However the spread was relatively large, with absolute values of Pearson's r taking values above >0.52 for leaf-level data (Fig. 4). We repeated this analysis with a GLS regression on re-centered and scaled species-mean data employing a Brownian phylogenetic correlation structure. In this case, all slope estimates (an approximate parallel to Pearson's r) took absolute values above 0.29 (Appendix S1: Table S1).

We also examined the predicted 1:1 relationship between $d_y/2$ and IVD. We found a positive relationship between these variables (SMA regression on log-transformed data; $R^2 = 0.35$, $P < 10^{-15}$). Observed data were close, but not equal, to the prediction of zero intercept and slope of unity (95% confidence interval for intercept, [−0.36, −0.13]; slope, [0.96, 1.08]) (Appendix S1: Fig. S5).

Phylogenetic patterns

Hierarchical variance decomposition indicated that VD and IVD were primarily determined at family level (≥39% variation), while thickness and vein radius were primarily determined at species or intraspecific levels (more than 26% variation) (Fig. 5).

There was wide variation in traits across the phylogenetic tree (Fig. 6). In general, the lowest values of VD were found amongst the Clusiaceae, and the highest among the Fabaceae, Urticaceae, and Moraceae, while the opposite was true for IVD. The lowest values of r_v and d_y were found consistently among the Fabaceae, while the highest values of r_v and d_y were found among the Clusiaceae.

Most traits varied more rapidly than under a Brownian motion model (Blomberg et al. 2003). The K value for VD was 0.90; for IVD, 1.32, for r_v, 0.47, for d_y, 0.43 (all $P \leq 0.002$). This result is consistent with limited evolutionary constraints on most venation network traits.

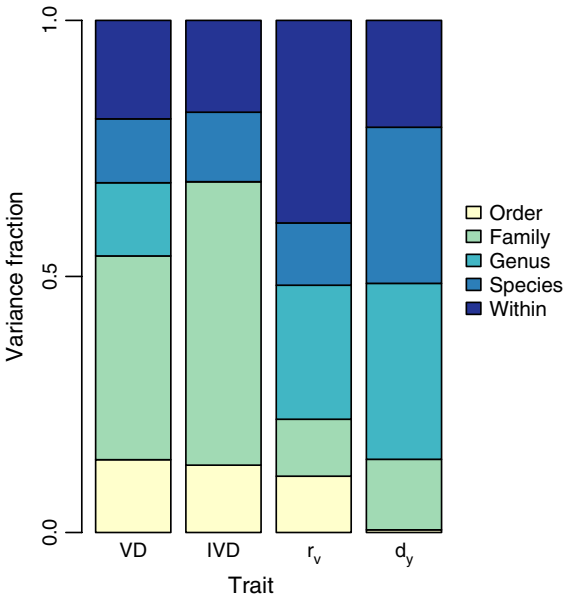

FIG. 5. Variance decomposition for venation network traits. Fractional bar lengths indicate variance partitioned at each taxonomic scale. [Colour figure can be viewed at wileyonlinelibrary.com]

Community-scale patterns

At community scale, abundance-weighted trait means showed correlations with climate. The strongest relationships were observed for temperature (all R^2 >0.45, $P < 0.05$), with warmer sites associated with higher VD, smaller r_v, lower d_y, and higher K_{est} (Fig. 7). Relationships with α PET_{max} also existed (all R^2 >0.5, $P < 0.05$, with higher water demand associated with higher VD, smaller r_v, lower d_y, and higher E_{max}. No relationships were observed between any trait variable and $\log_{10}$ precipitation ($P > 0.05$). This latter result is unsurprising given the high precipitation at all sites and likely lack of water limitation. However, there was a clear division in sites, with low evapotranspiration occurring at sites in the cloud immersion zone (above 1,500 m) and high evapotranspiration occurring below sites outside this zone.

We also repeated this analysis for only sun leaves and for only shade leaves. Results were broadly consistent with the complete dataset (sun leaves; Appendix S1: Fig. S6; shade leaves, Appendix S1: Fig. S7). Shade leaves showed stronger relationships than seen in the complete dataset. For example, the R^2 value for the mean annual temperature – VD relationship increased from 0.50 to 0.80, and the R^2 value for the E_{max} and α PET_{max} relationship increased from 0.41 to 0.59. However, this stratified analysis is potentially biased because some common species had canopies with no sun leaves or no shade leaves and as a result only contributed to the community-weighted trait in some cases. Nevertheless,

TER predictions

The TER model predicted a 1:1 relationship between E_{max} and α PET_{max}. Observations differed from the 1:1 expectation ($R^2 = 0.41$, $P = 0.046$, root mean square error of prediction, 1.06 mmol m^{-2} s^{-1}). However, both estimated coefficients overlapped the expectation of zero intercept and slope of unity (95% confidence interval for intercept, [−10.2, 3.3]; for slope, 0.0, 1.8]) (Fig. 8). Uncertainty due to unmeasured variation in $\Delta\Psi_{ls}$ and C_y/C_x was also important, with mean interquartile range variation in predicted values of E_{max} of 3.2 ± 1.3 mmol m^{-2} s^{-1}. While bias in these non-venation parameters could limit the power of the overall analysis, this bias would be insufficient to reject a positive relationship between E_{max} and α PET_{max}. Thus, the overall model was strictly falsified due to underestimation of E_{max}, but the relationship between these variables that was of the correct directionality and of approximately the correct magnitude.

We also assessed whether E_{max} increased with α PET_{max} within individual species. Because of high beta diversity along the gradient, only 8 species had measurements of E_{max} at more than two sites and none at more than four (Appendix S1: Fig. S8). Of these, 2/8 had slopes that were significantly greater than zero ($P < 0.05$) and 1/8 had a slope that was significantly less than zero.

DISCUSSION

While patterns for VD and IVD have been reported across climate gradients at regional scale for small sets of species (Uhl and Mosbrugger 1999, Kessler et al. 2007, Blonder et al. 2016) or globally in a meta-analysis (Sack and Scoffoni 2013), descriptions at the community scale are rare (Blonder and Enquist 2014). Our results, collected at the community scale in an understudied tropical ecosystem, support the consensus trend of increasing VD and decreasing IVD, r_v, and d_y at lower elevations and higher temperatures. These traits were integrated such that their combined effect on E_{max} also led to strong TERs. The lack of phylogenetic signal in all traits, as evidenced by low Blomberg's K values and non-zero phylogenetic regression slopes, suggests that these TERs are not likely to be driven by biogeographic constraints on the distributions of different clades along the elevation gradient. Rather, our results suggest that climate plays a strong mechanistic role in constraining trait values and thus the occurrence patterns of these angiosperm species. This constrasts with many of the TERs underlying paleoclimate reconstruction approaches (e.g., Wilf 1997, Little et al. 2010). The empirical TERs we report for VD, IVD, d_y, and r_v, advance understandings of trait coordination across environments and may be useful for paleoclimate reconstruction and community assembly studies. They also provide novel measurements for a wide set of tropical rainforest taxa from the Andean and Amazonian region.

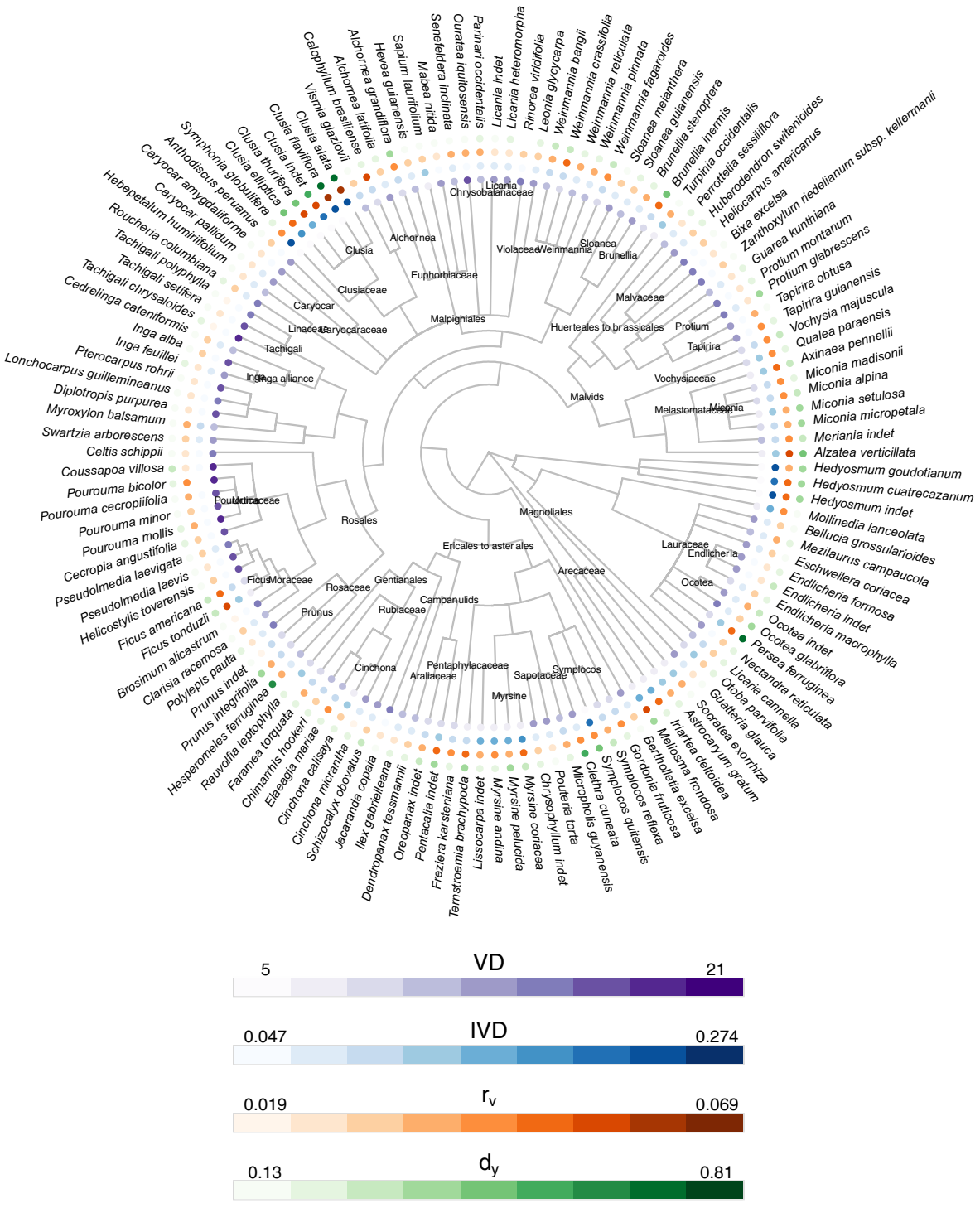

FIG. 6. Phylogenetic relationships among taxa. Circles for each species are shaded by trait value.

Within this trait correlation network, the negative relationship between VD and d_y has been previously hypothesized based on optimal flow arguments (Noblin et al. 2008). Subsequent critical examination has revealed inconsistent results (Blonder et al. 2011, Sack et al. 2013, Buckley et al. 2015). However, this study now provides evidence that this correlation is also found in Andean and Amazonian species, when using leaf half-thickness is a proxy for the minimum distance between vein and epidermis. Also, the negative relationship observed between

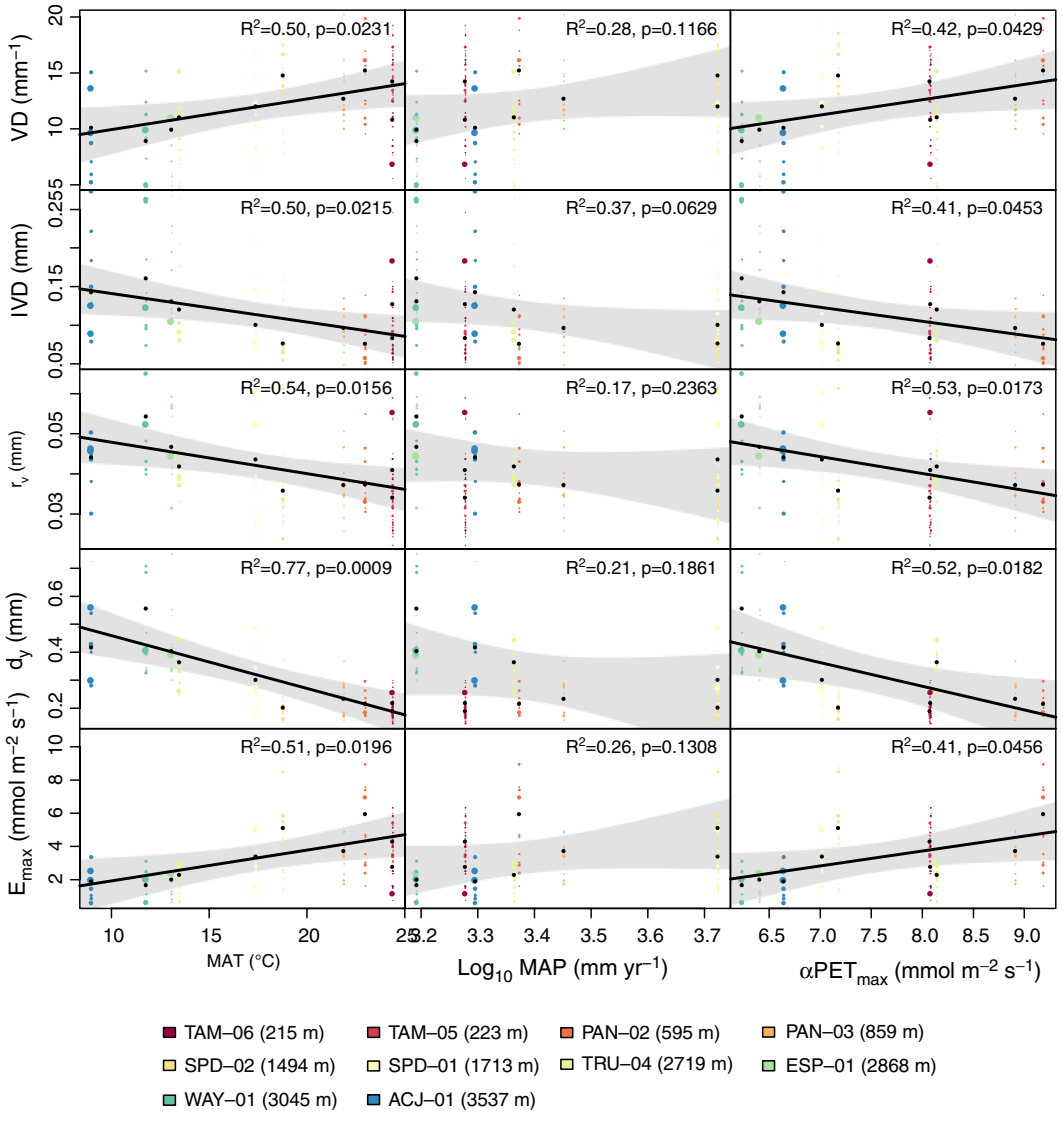

FIG. 7. Empirical trait-environment relationships. Points represent individual species and are shaded by plot elevation and sized by local abundance as measured by summed basal area. Regression 95% confidence intervals are shown in gray.

VD and r_v indicates integration of venation traits consistent with the findings of other phylogenetically broad studies (Sack et al. 2012, Feild and Brodribb 2013). This correlation is reasonable based on space-filling constraints: if a leaf reaches 1/VD = r_v, then the veins will overlap each other (Fig. 1). This may have implications for the relationship between carbon gain and carbon cost in leaves, as total vein density may predict photosynthetic rate and total vein volume may predict construction costs (Brodribb et al. 2007, Blonder et al. 2011, Sack and Scoffoni 2013).

The lack of difference in venation network traits between sun and shade leaves we observed was surprising. Several previous studies (reviewed in Sack and Scoffoni 2013) have found increased VD in sun leaves. A lack of difference has been observed in *Nothofagus*, but only at high elevations in trees with small crowns (Brodribb and Jordan 2011). This suggests that leaves nominally determined to be shaded or sunlit may actually experience similar microclimate conditions. However, this is unlikely to explain patterns in this elevation gradient, where quantitative light logger data has shown sunlit leaves are sunnier (A. Shenkin, *personal communication*). It is possible that long-lived leaves that were shaded at the time of collection were sunlit when they developed, but we did not have data to examine this possibility. Alternatively there may be less plasticity in vein density in these species than has been seen elsewhere.

The theory we tested has some utility for constructing hypotheses about TERs and community assembly.

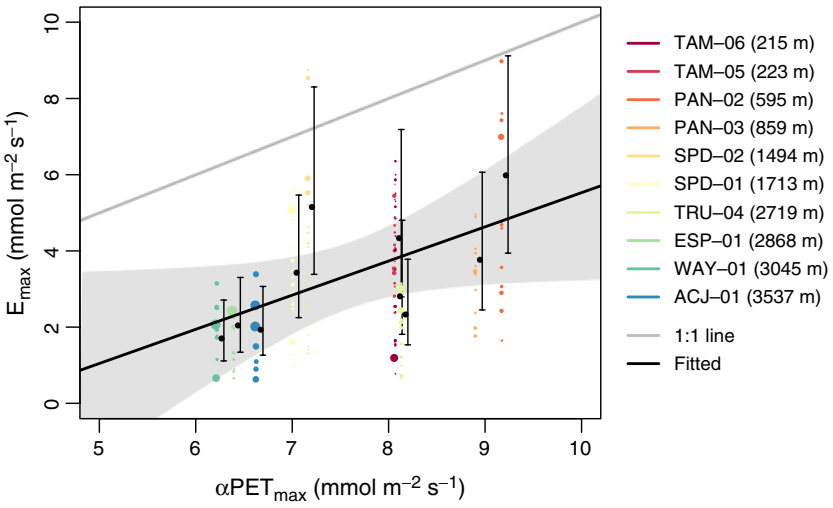

FIG. 8. Test of the prediction that maximum abundance-weighted mean transpiration (E_{max}) is equal to maximum potential evapotranspiration (α PET_{max}). Abundance-weighted mean values of E_{max} at each site take distributions that reflect propagated uncertainty due to leaf-stem water potential gradient $\Delta\Psi_{ls}$ and cell elongation ratio C_y/C_x: black dots indicate medians and bars indicate 25% and 75% quantiles. Points represent medians for individual species and are shaded by plot elevation and sized by local abundance as measured by summed basal area. The 1:1 prediction is shown as a gray line; linear regression through median E_{max} values is shown as a solid black line with gray 95% prediction confidence envelope.

Predictions for the relationships between site-scale climate and leaf-scale traits were of the correct sign and slope relative to observed data. However, the model systematically underestimated the data, and the relationship between VD and MAT was statistically stronger than the proposed relationship between E_{max} and α PET_{max}. This lack of model congruence with data may arise from five possible causes.

First, the parameterization of the model may have been imprecise. Unmeasured variation in parameters could have shifted model predictions. Specifically, if values of $\Delta\Psi_{ls}$ were higher than proposed and values of C_y/C_x were lower than proposed, predictions for E_{max} could be higher, resulting in better model fit. However, we found that variation in these parameters within their assumed ranges of uncertainty would only sometimes yield values that would overlap the 1:1 prediction line for E_{max} and α PET_{max}.

Second, the model for conductance may be too simple. Conductance also depends on other anatomical features such as bundle sheath extensions and sclereids (Brodribb et al. 2007, Sack and Scoffoni 2013, Buckley et al. 2015), as well as instantaneous transpiration rate and temperature (Buckley et al. 2015, Simonin et al. 2015). While the Brodribb et al. (2007) model provides a good fit to a phylogenetically broad sample of species, more detailed modeling of conductance could potentially further improve it. However, these anatomical traits are very time-intensive to measure, so that detailed information for several hundred species likely will remain out of reach for studies focused on community assembly.

Third, not all species in the community will experience the same value of α PET_{max}, as implicitly assumed. Variation in the environment among individuals (e.g., shaded canopies) could weaken the community-mean relationship even though relationships at individual scale might still be strong. Previous studies have demonstrated venation network trait differences between sun and shade leaves (reviewed in Sack and Scoffoni 2013). In this dataset, we found sun-shade differences in some venation network traits, and evidence for stronger TERs within shade and sun leaves compared to within the entire dataset. However, we did not find consistent evidence intraspecific venation network TERs, despite evidence for these in other systems (Blonder et al. 2013, 2015). However, the, high Andean beta diversity and the taxonomic breadth of our study necessarily led to limited within-species replication. Thus it seems possible that measuring microclimate variation may help to improve the strength abundance-weighted TERs.

Fourth, the model's assumption about leaf-scale transpiration matching (Eq. 10) may not hold for species that have conservative water-use strategies. However, the high precipitation (>1,500 mm yr^{-1}) at all communities suggests that these strategies are unlikely here. Selection may not be occurring on hydraulic capacity, but instead on hydraulic vulnerability. A previous study on evergreen angiosperms in the same Peruvian environments showed that species' climatic limits are consistent with linkages between hydraulic vulnerability and rainfall (Blackman et al. 2011). Hydraulic capacity may therefore be an important, but not complete, predictor of environmental filtering.

Fifth, the underlying data for potential evapotranspiration may have been limited. Data were only available for 1 yr and may not have been representative of the long-term

means and extremes that constrain the distribution of species in this gradient. Both interannual variation and differences in cloud immersion along the gradient are likely to play an important and unmeasured role in evapotranspiration in these sites by altering vapor pressure deficit and suppressing transpiration (Gotsch et al. 2016) or by altering the water available for (and the direction of) hydraulic conductance through the direct uptake of water through leaves (Goldsmith et al. 2013). Leaf-level, whole plant and ecosystem transpiration are known to vary along tropical montane elevation gradients where cloudiness plays a considerable role (Gotsch et al. 2016). This may provide an explanation for why several TERs demonstrated abrupt jumps in trait values at the cloud boundary. However, the role of clouds was not directly examined here beyond their effects on microclimate (e.g., vapor pressure deficit, temperature, and insolation) for statistical reasons because of the high covariation between temperature and cloudiness in this system.

Taken as a whole, the utility of the Blonder and Enquist (2014) model for quantitatively predicting TERs remains tentative but promising: predictions of the TER slope are correct, but predictions for the TER intercept are biased. The observation that any correlations are observed at all, despite the data challenges and approximations inherent to broad comparative studies, suggests that the model deserves further examination. Quantitative theories are by their nature easy to falsify, but falsified predictions indicate a need to refine theory, refine data, or propose alternatives. Doing any of these remains an ongoing and important challenge.

We have shown that a number of traits linked to leaf venation networks are coordinated with each other and with climate gradients, leading to strong abundance-weighted TERs, and that at the community scale, the empirical TER between abundance-weighted maximum transpiration rate (as modeled using venation network traits) and potential evapotranspiration was close, but not equal, to the 1:1 prediction. These results offer an empirical perspective on the drivers of leaf traits across an Andes-Amazon elevation gradient and also highlight the challenges inherent to developing trait-based climate reconstruction and community assembly.

Acknowledgments

This work is a product of the Global Ecosystems Monitoring (GEM) network (gem.tropicalforests.ox.ac.uk) the Andes Biodiversity and Ecosystems Research Group ABERG (andes-research.org), the Amazon Forest Inventory Network RAINFOR (www.rainfor.org), and the Carnegie Spectranomics Project (spectranomics.carnegiescience.edu) research consortia. The field campaign was funded by grants to Yadvinder Malhi from the UK Natural Environment Research Council (Grant NE/J023418/1), with additional support from European Research Council advanced investigator grants GEM-TRAITS (321131), T-FORCES (291585), and a John D. and Catherine T. MacArthur Foundation grant to Gregory Asner. We thank the Servicio Nacional de Áreas Naturales Protegidas por el Estado (SERNANP) and personnel of Manu and Tambopata National Parks for logistical assistance and permission to work in the protected areas. We also thank the Explorers' Inn and the Pontifical Catholic University of Peru, as well as ACCA for use of the Tambopata and Wayqecha Research Stations, respectively. Professor Eric Cosio (Pontifical Catholic University of Peru) provided assistance with research permissions and sample analysis and storage. Taxonomic work at Carnegie Institution was facilitated by Raul Tupayachi, Felipe Sinca, and Nestor Jaramillo. Clarke Knight made vein radius measurements. Benjamin Blonder was supported by a United States National Science Foundation graduate research fellowship and doctoral dissertation improvement grant DEB-1209287, as well as a UK Natural Environment Research Council independent research fellowship NE/M019160/1. Gregory Asner and the Spectranomics team were supported by the endowment of the Carnegie Institution for Science and a grant from the National Science Foundation (DEB-1146206). Brian J. Enquist was supported by the National Science Foundation (Macrosystems-1065861 and DEB-1457812). Yadvinder Malhi was supported by the Jackson Foundation. Sandra Díaz was supported by the Leverhulme Trust (UK), the Inter-American Institute for Global Change Research, and FONCyT and CONICET (Argentina). Gregory Goldsmith was supported by funding from the European Community's Seventh Framework Program (FP7/2007–2013) under grant agreement 290605 (COFUND: PSI-FELLOW). Cyrille Violle was supported by a Marie Curie International Outgoing Fellowship within the 7th European Community Framework Program (DiversiTraits project, no. 221060) and by the European Research Council (ERC) Starting Grant Project StG-2014-639706-CONSTRAINTS. We thank several anonymous reviewers for comments that greatly improved the manuscript.

Literature Cited

Allen, R. G., L. S. Pereira, D. Raes, and M. Smith. 1998. Crop evapotranspiration-Guidelines for computing crop water requirements-FAO Irrigation and drainage paper 56. FAO, Rome 300:D05109.

Arnold, S. J. 1983. Morphology, performance and fitness. American Zoologist 23:347–361.

Bailey, I., and E. Sinnott. 1915. A botanical index of Cretaceous and Tertiary climates. Science 41:831–834.

Bartlett, M. K., C. Scoffoni, and L. Sack. 2012. The determinants of leaf turgor loss point and prediction of drought tolerance of species and biomes: a global meta-analysis. Ecology Letters 15:393–405.

Blackman, C. J., T. J. Brodribb, and G. J. Jordan. 2011. Leaf hydraulic vulnerability influences species' bioclimatic limits in a diverse group of woody angiosperms. Oecologia 168: 1–10.

Blomberg, S. P., T. Garland, A. R. Ives, and B. Crespi. 2003. Testing for phylogenetic signal in comparative data: behavioral traits are more labile. Evolution 57:717–745.

Blonder, B., and B. J. Enquist. 2014. Inferring climate from angiosperm leaf venation networks. New Phytologist 204: 116–126.

Blonder, B., C. Violle, L. P. Bentley, and B. J. Enquist. 2011. Venation networks and the origin of the leaf economics spectrum. Ecology Letters 14:91–100.

Blonder, B., et al. 2012. The leaf-area shrinkage effect can bias paleoclimate and ecology research. American Journal of Botany 99:1756–1763.

Blonder, B., C. Violle, and B. J. Enquist. 2013. Assessing the causes and scales of the leaf economics spectrum using venation networks in *Populus tremuloides*. Journal of Ecology 101:981–989.

Blonder, B., F. Vasseur, C. Violle, B. Shipley, B. J. Enquist, and D. Vile. 2015. Testing models for the leaf economics spectrum with leaf and whole-plant traits in *Arabidopsis thaliana*. Annals of Botany: Plants 7:plv049.

Blonder, B., B. G. Baldwin, B. J. Enquist, and R. H. Robichaux. 2016. Variation and macroevolution in leaf functional traits in the Hawaiian silversword alliance (Asteraceae). Journal of Ecology 104:219–228.

de Boer, H. J., M. B. Eppinga, M. J. Wassen, and S. C. Dekker. 2012. A critical transition in leaf evolution facilitated the Cretaceous angiosperm revolution. Nature Communications 3:1221.

Boyce, C. K., T. Brodribb, T. S. Feild, and M. A. Zwieniecki. 2009. Angiosperm leaf vein evolution was physiologically and environmentally transformative. Proceedings of the Royal Society B 276:1771–1776.

Brodribb, T., and T. S. Feild. 2010. Leaf hydraulic evolution led a surge in leaf photosynthetic capacity during early angiosperm diversification. Ecology Letters 13:175–183.

Brodribb, T., and G. Jordan. 2011. Water supply and demand remain balanced during leaf acclimation of *Nothofagus cunninghamii* trees. New Phytologist 192:437–448.

Brodribb, T. J., N. M. Holbrook, and M. V. Gutiérrez. 2002. Hydraulic and photosynthetic co-ordination in seasonally dry tropical forest trees. Plant, Cell and Environment 25: 1435–1444.

Brodribb, T., T. Feild, and G. Jordan. 2007. Leaf maximum photosynthetic rate and venation are linked by hydraulics. Plant Physiology 144:1890.

Buckley, T. N., G. P. John, C. Scoffoni, and L. Sack. 2015. How does leaf anatomy influence water transport outside the xylem? Plant Physiology 168:1616–1635.

Choné, X., C. Van Leeuwen, D. Dubourdieu, and J. P. Gaudillère. 2001. Stem water potential is a sensitive indicator of grapevine water status. Annals of Botany 87:477–483.

Cingolani, A. M., M. Cabido, D. E. Gurvich, D. Renison, and S. Díaz. 2007. Filtering processes in the assembly of plant communities: Are species presence and abundance driven by the same traits? Journal of Vegetation Science 18:911–920.

Cody, M. L., and J. M. Diamond. 1975. Ecology and evolution of communities. Harvard University Press, Cambridge, Massachusetts, USA.

Connor, E. F., and D. Simberloff. 1979. The assembly of species communities: Chance or competition? Ecology 60:1132–1140.

Craine, J. 2009. Resource strategies of wild plants. Princeton University Press, Princeton, New Jersey, USA.

Díaz, S., M. Cabido, and F. Casanoves. 1998. Plant functional traits and environmental filters at a regional scale. Journal of Vegetation Science 9:113–122.

Edwards, E. J., D. S. Chatelet, L. Sack, and M. J. Donoghue. 2014. Leaf life span and the leaf economic spectrum in the context of whole plant architecture. Journal of Ecology 102:328–336.

Elser, J. J., W. F. Fagan, A. J. Kerkhoff, N. G. Swenson, and B. J. Enquist. 2010. Biological stoichiometry of plant production: metabolism, scaling and ecological response to global change. New Phytologist 186:593–608.

Ephrath, J. E., J. Goudriaan, and A. Marani. 1996. Modelling diurnal patterns of air temperature, radiation wind speed and relative humidity by equations from daily characteristics. Agricultural Systems 51:377–393.

Feild, T. S., and T. Brodribb. 2013. Hydraulic tuning of vein cell microstructure in the evolution of angiosperm venation networks. New Phytologist 199:720–726.

Franks, P. J. 2006. Higher rates of leaf gas exchange are associated with higher leaf hydrodynamic pressure gradients. Plant, Cell and Environment 29:584–592.

Fukami, T. 2015. Historical contingency in community assembly: integrating niches, species pools, and priority effects. Annual Review of Ecology, Evolution, and Systematics 46: 1–23.

Fyllas, N. M., et al. 2014. Analysing Amazonian forest productivity using a new individual and trait-based model (TFS v.1). Geoscientific Model Development 7:1251–1269.

Fyllas, N. M., et al. submitted. Solar radiation and functional traits are both necessary and sufficient to explain the decline of forest primary productivity along a tropical elevation gradient. Ecology Letters.

Gastauer, M., and J. A. A. Meira-Neto. 2013. Avoiding inaccuracies in tree calibration and phylogenetic community analysis using Phylocom 4.2. Ecological Informatics 15:85–90.

Girardin, C., Y. Malhi, K. Feeley, J. Rapp, M. Silman, P. Meir, W. Huaraca Huasco, N. Salinas, M. Mamani, and J. Silva-Espejo. 2014*a*. Seasonality of above-ground net primary productivity along an Andean altitudinal transect in Peru. Journal of Tropical Ecology 30:503–519.

Girardin, C. A., W. Farfan-Rios, K. Garcia, K. J. Feeley, P. M. Jørgensen, A. A. Murakami, L. Cayola Pérez, R. Seidel, N. Paniagua, and A. F. Fuentes Claros. 2014*b*. Spatial patterns of above-ground structure, biomass and composition in a network of six Andean elevation transects. Plant Ecology and Diversity 7:161–171.

Goldsmith, G. R., N. J. Matzke, and T. E. Dawson. 2013. The incidence and implications of clouds for cloud forest plant water relations. Ecology Letters 16:307–314.

Gotsch, S. G., H. Asbjornsen, and G. R. Goldsmith. 2016. Plant carbon and water fluxes in tropical montane cloud forests. Journal of Tropical Ecology 32:404–420.

Halladay, K., Y. Malhi, and M. New. 2012. Cloud frequency climatology at the Andes/Amazon transition: 1. Seasonal and diurnal cycles. Journal of Geophysical Research: Atmospheres 117:D23.

Hinojosa, L. F., F. Pérez, A. Gaxiola, and I. Sandoval. 2011. Historical and phylogenetic constraints on the incidence of entire leaf margins: insights from a new South American model. Global Ecology and Biogeography 20:380–390.

Houlahan, J. E.. 2016. The priority of prediction in ecological understanding. Oikos 126:1–7.

Jackson, S. T., and J. T. Overpeck. 2000. Responses of plant populations and communities to environmental changes of the late Quaternary. Paleobiology 26:194–220.

Jordan, G. 2011. A critical framework for the assessment of biological palaeoproxies: predicting past climate and levels of atmospheric CO2 from fossil leaves. New Phytologist 192: 29–44.

Kessler, M., Y. Siorak, M. Wunderlich, and C. Wegner. 2007. Patterns of morphological leaf traits among pteridophytes along humidity and temperature gradients in the Bolivian Andes. Functional Plant Biology 34:963–971.

Lavorel, S., and E. Garnier. 2002. Predicting changes in community composition and ecosystem functioning from plant traits: revisiting the Holy Grail. Functional Ecology 16: 545–556.

Levins, R. 1966. The strategy of model building in population biology. American Scientist 54:421–431.

Levins, R., and R. C. Lewontin. 1985. The dialectical biologist. Harvard University Press, Cambridge, Massachusetts, USA.

Little, S. A., S. W. Kembel, and P. Wilf. 2010. Paleotemperature proxies from leaf fossils reinterpreted in light of evolutionary history. PLoS ONE 5:e15161.

Malhi, Y., M. Silman, N. Salinas, M. Bush, P. Meir, and S. Saatchi. 2010. Introduction: Elevation gradients in the tropics: laboratories for ecosystem ecology and global change research. Global Change Biology 16:3171–3175.

Manzoni, S., G. Vico, A. Porporato, and G. Katul. 2013. Biological constraints on water transport in the soil–plant–atmosphere system. Advances in Water Resources 51: 292–304.

Marquet, P. A., et al. 2014. On theory in ecology. BioScience 64:701–710.

Martínez-Vilalta, J., R. Poyatos, D. Aguadé, J. Retana, and M. Mencuccini. 2014. A new look at water transport regulation in plants. New Phytologist 204:105–115.

Mason, C. M., and L. A. Donovan. 2015. Evolution of the leaf economics spectrum in herbs: evidence from environmental divergences in leaf physiology across Helianthus (Asteraceae). Evolution 69:2705–2720.

McGill, B., B. Enquist, E. Weiher, and M. Westoby. 2006. Rebuilding community ecology from functional traits. Trends in Ecology & Evolution 21:178–185.

Messier, J., B. J. McGill, and M. J. Lechowicz. 2010. How do traits vary across ecological scales? A case for trait-based ecology. Ecology Letters 13:838–848.

Moles, A. T., et al. 2014. Which is a better predictor of plant traits: temperature or precipitation? Journal of Vegetation Science 25:1167–1180.

Noblin, X., L. Mahadevan, I. A. Coomaraswamy, D. A. Weitz, N. M. Holbrook, and M. A. Zwieniecki. 2008. Optimal vein density in artificial and real leaves. Proceedings of the National Academy of Sciences of the United States of America 105:9140–9144.

Paine, C. E. T., C. Baraloto, and S. Díaz. 2015. Optimal strategies for sampling functional traits in species-rich forests. Functional Ecology 29:1325–1331.

Peppe, D. J., D. L. Royer, B. Cariglino, S. Y. Oliver, S. Newman, E. Leight, G. Enikolopov, M. Fernandez-Burgos, F. Herrera, and J. M. Adams. 2011. Sensitivity of leaf size and shape to climate: global patterns and paleoclimatic applications. New Phytologist 190:724–739.

Pérez-Harguindeguy, N., S. Díaz, E. Garnier, S. Lavorel, H. Poorter, P. Jaureguiberry, M. Bret-Harte, W. Cornwell, J. Craine, and D. Gurvich. 2013. New handbook for standardised measurement of plant functional traits worldwide. Australian Journal of Botany 61:167–234.

Priestley, C. H. B., and R. J. Taylor. 1972. On the assessment of surface heat flux and evaporation using large-scale parameters. Monthly Weather Review 100:81–92.

Read, Q. D., L. C. Moorhead, N. G. Swenson, J. K. Bailey, and N. J. Sanders. 2014. Convergent effects of elevation on functional leaf traits within and among species. Functional Ecology 28:37–45.

Reich, P. B. 2014. The world-wide 'fast–slow' plant economics spectrum: a traits manifesto. Journal of Ecology 102:275–301.

Reich, P., D. Ellsworth, M. Walters, J. Vose, C. Gresham, J. Volin, and W. Bowman. 1999. Generality of leaf trait relationships: a test across six biomes. Ecology 80: 1955–1969.

Rockwell, F. E., N. Michele Holbrook, and A. D. Stroock. 2014. Leaf hydraulics II: vascularized tissues. Journal of Theoretical Biology 340:267–284.

Roth-Nebelsick, A., D. Uhl, V. Mosbrugger, and H. Kerp. 2001. Evolution and function of leaf venation architecture: a review. Annals of Botany 87:553–566.

Royer, D., and P. Wilf. 2006. Why do toothed leaves correlate with cold climates? Gas exchange at leaf margins provides new insights into a classic paleotemperature proxy. International Journal of Plant Sciences 167:11–18.

Royer, D., P. Wilf, D. Janesko, E. Kowalski, and D. Dilcher. 2005. Correlations of climate and plant ecology to leaf size and shape: potential proxies for the fossil record. American Journal of Botany 92:1141.

Sack, L., and N. M. Holbrook. 2006. Leaf hydraulics. Annual Review of Plant Biology 57:361–381.

Sack, L., and C. Scoffoni. 2013. Leaf venation: structure, function, development, evolution, ecology and applications in the past, present and future. New Phytologist 198:983–1000.

Sack, L., C. Scoffoni, A. D. Mckown, K. Frole, M. Rawls, J. C. Havran, H. Tran, and T. Tran. 2012. Developmentally based scaling of leaf venation architecture explains global ecological patterns. Nature Communications 3:837.

Sack, L., C. Scoffoni, G. P. John, H. Poorter, C. M. Mason, R. Mendez-Alonzo, and L. A. Donovan. 2013. How do leaf veins influence the worldwide leaf economic spectrum? Review and synthesis. Journal of Experimental Botany 64: 4053–4080.

Scheiter, S., L. Langan, and S. I. Higgins. 2013. Next-generation dynamic global vegetation models: learning from community ecology. New Phytologist 198:957–969.

Shipley, B., D. Vile, and É. Garnier. 2006. From plant traits to plant communities: a statistical mechanistic approach to biodiversity. Science 314:812–814.

Simonin, K. A., E. Burns, B. Choat, M. M. Barbour, T. E. Dawson, and P. J. Franks. 2015. Increasing leaf hydraulic conductance with transpiration rate minimizes the water potential drawdown from stem to leaf. Journal of Experimental Botany 66:1303–1315.

Suding, K. N., S. Lavorel, F. S. Chapin, J. H. C. Cornelissen, S. Díaz, E. Garnier, D. Goldberg, D. U. Hooper, S. T. Jackson, and M.-L. Navas. 2008. Scaling environmental change through the community-level: a trait-based response-and-effect framework for plants. Global Change Biology 14:1125–1140.

Thornley, J. H. M. 1991. A transport-resistance model of forest growth and partitioning. Annals of Botany 68:211–226.

Tyree, M. T., and J. S. Sperry. 1988. Do woody plants operate near the point of catastrophic xylem dysfunction caused by dynamic water stress? Answers from a model. Plant Physiology 88:574–580.

Uhl, D., and V. Mosbrugger. 1999. Leaf venation density as a climate and environmental proxy: a critical review and new data. Palaeogeography, Palaeoclimatology, Palaeoecology 149:15–26.

Umaña, M. N., C. Zhang, M. Cao, L. Lin, and N. G. Swenson. 2015. Commonness, rarity, and intraspecific variation in traits and performance in tropical tree seedlings. Ecology Letters 18:1329–1337.

Vellend, M., and A. Agrawal. 2010. Conceptual synthesis in community ecology. The Quarterly Review of Biology 85: 183–206.

Violle, C., P. B. Reich, S. W. Pacala, B. J. Enquist, and J. Kattge. 2014. The emergence and promise of functional biogeography. Proceedings of the National Academy of Sciences 111: 13690–13696.

Webb, C. O., D. D. Ackerly, and S. W. Kembel. 2008. Phylocom: software for the analysis of phylogenetic community structure and trait evolution. Bioinformatics 24: 2098–2100.

Weiher, E., and P. A. Keddy. 1999. Ecological assembly rules: perspectives, advances, retreats. Cambridge University Press, Cambridge, UK.

Weiher, E., D. Freund, T. Bunton, A. Stefanski, T. Lee, and S. Bentivenga. 2011. Advances, challenges and a developing synthesis of ecological community assembly theory. Philosophical Transactions of the Royal Society B: Biological Sciences 366:2403–2413.

Wikström, N., V. Savolainen and M. W. Chase. 2001. Evolution of the angiosperms: calibrating the family tree. Proceedings of the Royal Society of London. Series B: Biological Sciences 268:2211–2220.

Wilf, P. 1997. When are leaves good thermometers? A new case for leaf margin analysis. Paleobiology 23:373–390.

Wolfe, J. 1993. A method of obtaining climatic parameters from leaf assemblages. USGS Bulletin 2040:1–75.

Wright, I., P. Reich, M. Westoby, D. Ackerly, Z. Baruch, F. Bongers, J. Cavender-Bares, T. Chapin, J. Cornelissen, and M. Diemer. 2004. The worldwide leaf economics spectrum. Nature 428:821–827.

Wright, I. J., P. B. Reich, J. H. Cornelissen, D. S. Falster, P. K. Groom, K. Hikosaka, W. Lee, C. H. Lusk, Ü. Niinemets, and J. Oleksyn. 2005. Modulation of leaf economic traits and trait relationships by climate. Global Ecology and Biogeography 14:411–421.

Wylie, R. B. 1946. Relations between tissue organization and vascularization in leaves of certain tropical and subtropical dicotyledons. American Journal of Botany 33:721–726.

Supporting Information

Additional supporting information may be found in the online version of this article at http://onlinelibrary.wiley.com/doi/10.1002/ecy.1747/suppinfo